Contamination resistant antireflection nano-textures in fused silica for laser optics.

Douglas S. Hobbs*, Bruce D. MacLeod, Ernest Sabatino III

TelAztec LLC, 15 A Street, Burlington, MA, USA 01803-3404

Jerald A. Britten^, Christopher J. Stolz

Lawrence Livermore National Laboratory, POB 808 L-470, Livermore, CA 94551

ABSTRACT

Anti-reflecting (AR) surface relief nano-textures have been integrated with fused silica diffraction gratings to demonstrate the potential of stable diffractive 3ω beam samplers with increased energy to target at the National Ignition Facility (NIF). TelAztec's AR texturing process was used to etch Random-type AR (RAR) microstructures in sub-scale NIF Grating Debris Shields consisting of large pitch, shallow line gratings. This superposition yielded the desired ~3.5% increase in zero-order transmission uniformly over the full aperture without compromising the grating function. Another fused silica window fabricated with RAR nano-textures in both faces for a 3ω (351nm) transmission of 99.5%, was subjected to capillary condensation tests to evaluate the resistance of the RAR texture to the adsorption of organic compounds. It was found that for a one day exposure time to a surrogate suite of organic contaminants, the RAR textured fused silica surfaces adsorbed less than one fourth the amount of organic contaminants found on a NIF baseline hardened sol-gel AR coated optic. In two additional exposure cycles, further RAR process refinement reduced the amount of adsorbed organics to a level nearly 200 times below the current NIF baseline. Significantly, the 3ω transmission of the RAR textured window remained unchanged after all three exposure cycles, whereas the sol-gel coated windows showed losses up to 4.9% for the highest contaminant concentration. Large beam pulsed laser damage testing of RAR textured fused silica windows was conducted with the Optical Sciences Laser (OSL) at NIF. The RAR sample damage resistance was found to be equivalent to the current NIF baseline – even after multiple aggressive chemical cleaning cycles. Lastly, a series of RAR textured and sol-gel AR coated windows were subjected to commercial 3ω pulsed laser damage testing at Quantel. The results indicate an average RAR damage threshold of 26 J/cm^2, a level about 80% of the two NIF fused silica samples tested, two times higher than the best performing ion beam sputtered thin-film AR coatings reported in the literature, and six times higher than catalog high power laser window coating specifications.

Keywords: Nano-Textures, Anti-reflection, AR, Motheye, Laser Damage, Organic Adsorption, Sol-Gel Coatings, Grating Debris Shields

1.0 INTRODUCTION

Within the world's most powerful laser system being developed for fusion energy research by the Lawrence Livermore National Laboratory's (LLNL) National Ignition Facility (NIF), more than seven thousand optical components must transmit extremely high energy laser pulses at near infrared and near ultraviolet wavelengths.[1-3] To advance the operational lifetime of NIF optics, reduce operational costs, and further increase the laser output, surface treatment methods for increasing the laser damage resistance are being continuously pursued. Currently, anti-reflection (AR) coatings based on silica sol-gel materials provide good laser damage resistance and high transmission for fused silica optics,[4-8] but this resistance and transmission degrades rapidly due to the adsorption of organic materials from the environment.[9] In addition, low efficiency diffraction gratings like that shown in the scanning electron microscope (SEM) image on the right, are used in each of the 192 NIF beam lines for diagnostic purposes.[10,11] These gratings cannot be practically combined with sol-gel AR coating layers and therefore the amount of laser energy that can be delivered to the fusion target is reduced by 3.5% for each beam. To address these issues, the concept of replacing sol-gel thin-film AR coatings with surface relief microstructures etched directly into the fused silica optic material was investigated. It was anticipated that the nanometer (nm) scale features

45°

Fused Silica GDS 2µm 9000X
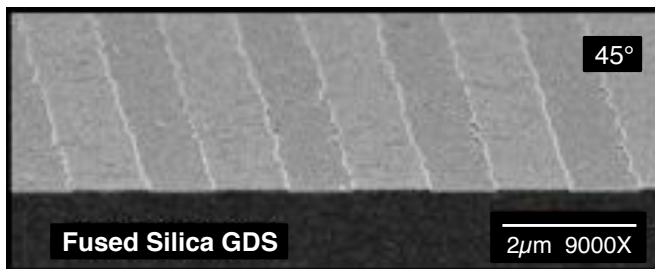
* dshobbs@telaztec.com; phone 1 781 229-9905; www.telaztec.com;   ^ britten1@llnl.gov; phone 1 925-423-7653

that make up a graded-index AR texture could be superimposed upon the micrometer (μm) scale diffraction grating features to eliminate the 3.5% transmission loss without compromising the grating function. And because TelAztec's Random-type AR (RAR) texture etched in glass materials has been observed to enhance the hydrophobic and oleophobic qualities of an optic, it was also anticipated that RAR textured optics might be more resistant to the adsorption of organic contaminants, further enabling their use on GDS optics.

2.0 BACKGROUND

2.1 Fused Silica Grating Debris Shields at the National Ignition Facility

A sketch of one of the 192 Final Optics Assemblies (FOA) at NIF, is shown in Figure 1 (as adapted from references 1 and 2).[1-2] Each FOA employs frequency converters to transform 1053nm wavelength laser light (known as 1ω at NIF) into 526.5nm (2ω) and then 351nm (UV, 3ω) light before focusing each beam onto the fusion target. In the latest configuration, the 3ω sampling grating optics also serve as debris shields (GDS) to protect upstream optics. GDS optics are 43 cm square planar fused silica windows with a full-aperture off-axis focusing grating imprinted into the output surface via laser interference lithography followed by wet etching. The binary grating has a pitch in the range of ~1600-2000nm, and is etched to a depth of about 20nm for a 1st order diffraction efficiency around 0.25% for 3ω light. Such low efficiency is needed to avoid saturating – or damaging – the imaging system detectors. The advantage of this geometry is that the sampling beam travels the same optical path as the main beam, but a requirement is that the intensity ratio of sampled to main beam remain constant. Sol-gel silica AR coatings applied as suspensions by dip, spin or meniscus coating, are used on all high-fluence transmissive optics in the NIF chain, including the input surface of the GDS. These coatings tend to planarize the GDS modulation as shown in the SEM cross section on the right. Due to the extremely high specific surface area and nano-porous structure of the sol-gel, adsorption of mainly organic contaminants from target debris gradually increases the refractive index of the sol-gel film. Taken together, these effects decrease the intensity ratio of sampled to main beam over time. Alternative thin-film AR coating materials are more environmentally stable than sol-gel coatings, but exhibit only a fraction of the laser damage resistance attained with sol-gels.[8] As a result, the current GDS optics trade signal stability for loss of throughput, and do not use any AR coatings on the grating surface. Recovering the 3.5% Fresnel loss per beam while maintaining signal stability is a priority on the NIF roadmap for achieving higher energy on target.[3]
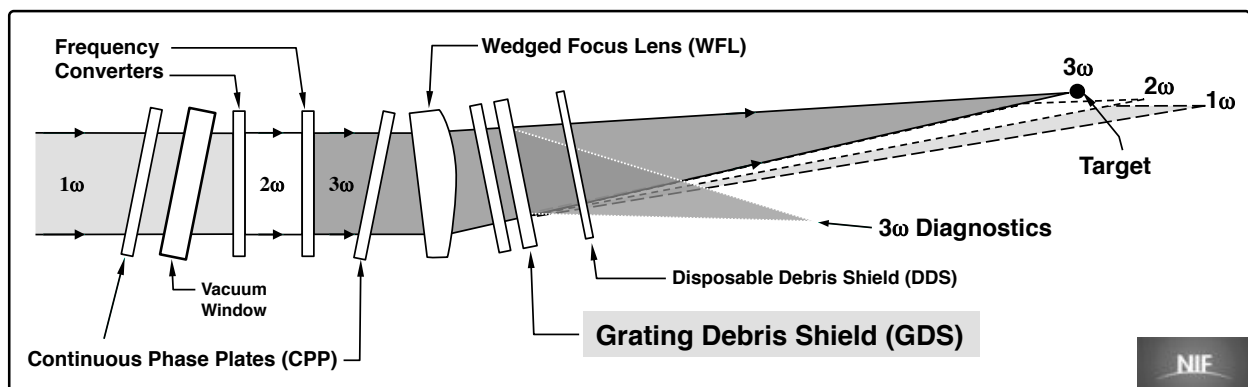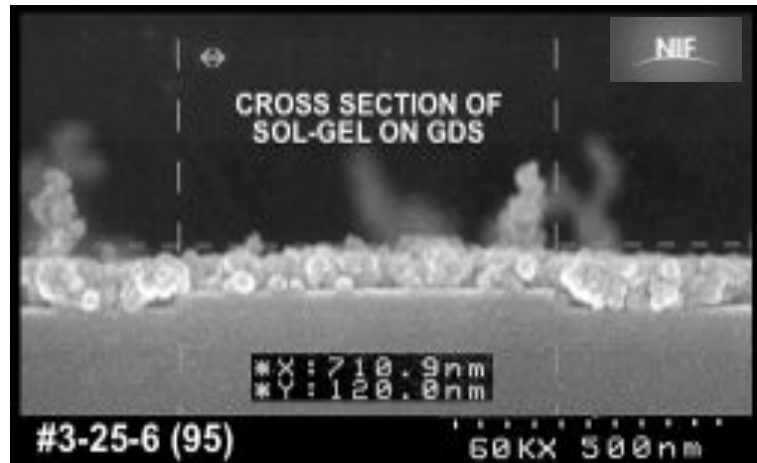
Figure 1: Concept diagram of the components within each Final Optics Assembly at NIF.

2.2 AR Microstructure Technology

As an effective replacement for sol-gel and other conventional thin-film AR coating materials, surface relief textures with sub wavelength scale features can be etched into bulk optic materials such as fused silica. When designed with smoothly varying – or analog feature profiles – these textures present a graded refractive index for propagating light with no abrupt interfaces to cause reflection losses. Motheye AR structures,[12-14] like the array of cones etched in diamond shown in the SEM on the right, are perhaps the most widely known optically functional texture. Motheye textures have been shown to exhibit high performance combined with the mechanical, optical, and chemical durability of the bulk material.[15-19]
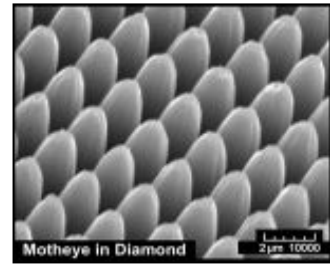
Motheye AR Microstructures (ARMs) are difficult to scale to very large area optics due to the pattern generation (lithography) requirement. Even using a laser based holographic or interference lithography[20] system, the production of high contrast Motheye pattern etch masks has a practical area limit of about 15 centimeter diameter.

For larger scale ARMs textures, TelAztec has developed a patented plasma-etch process to fabricate randomly distributed cone-like features directly from the reactive ions in the plasma, eliminating the lithography requirement.[13,17,19] Referred to as Random AR (RAR) textures, plasma-etch recipes have been developed for fused silica and glass materials, as well as for many other optical materials such as silicon and zinc selenide. An SEM image of an RAR texture in the surface of a zinc selenide window that transmits well at 1064nm, is shown on the right. The clear aperture of an optic that can be RAR treated is dependent only on the scale of the plasma etch tool, with common tool sizes ranging from 20-45cm round (8-18 inches). Figure 2 shows the 20cm tool in operation at TelAztec processing RAR textures in a batch of thirteen 1-inch round fused silica laser windows. Scaling to the 60cm round tool needed for 43cm square NIF optics is straight forward, but requires a custom built system.
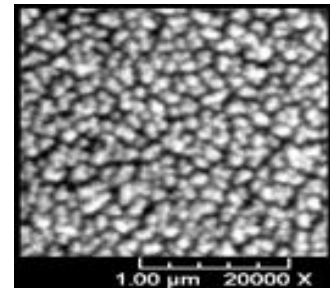
RAR textures in fused silica have exhibited huge bandwidths compared to thin-film AR coatings with peak reflection losses below 0.3% over the UV through NIR spectral range from 0.2 to 0.9µm, or the visible-NIR range of 0.4-2.0µm, with losses as low as 0.03% at selected wavelengths within the 0.6-1.55µm range.[19] A growing body of data has also shown high pulsed laser damage thresholds for RAR textures in fused silica and glass. Thresholds up to 5 times that of thin film AR coatings have been recorded in standardized testing at multiple wavelengths.[13,19]
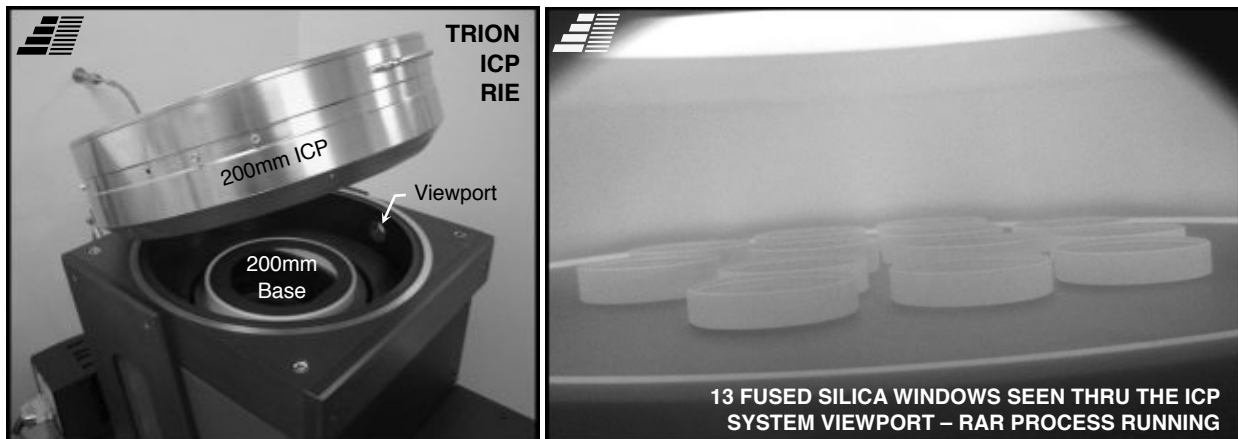

Figure 2: TelAztec's 20cm plasma etch tool (left), and a view into the chamber during a RAR texture batch process (right).

3.0 RAR FABRICATION AND MEASURED PERFORMANCE

As illustrated in the process flow diagram of Figure 3, RAR textures are fabricated using a sequence of steps that are quite similar to the steps for depositing thin-film AR coatings. One or more optics are first cleaned (1) and then placed into a carrier fixture (2) that is then loaded into the plasma etch tool vacuum chamber. A RAR etch recipe is then initiated under computer control (3). The etch recipe may include options such as a pre- or post-RAR argon or oxygen ion cleaning, and all etch parameters such as temperature, pressure, power, gas composition and gas flow rates are logged and maintained by the computer during the run. Typical cycle times for the 3ω fused silica optics discussed herein were about 20 minutes from load to unload (4) – much faster than typical coating deposition cycles.
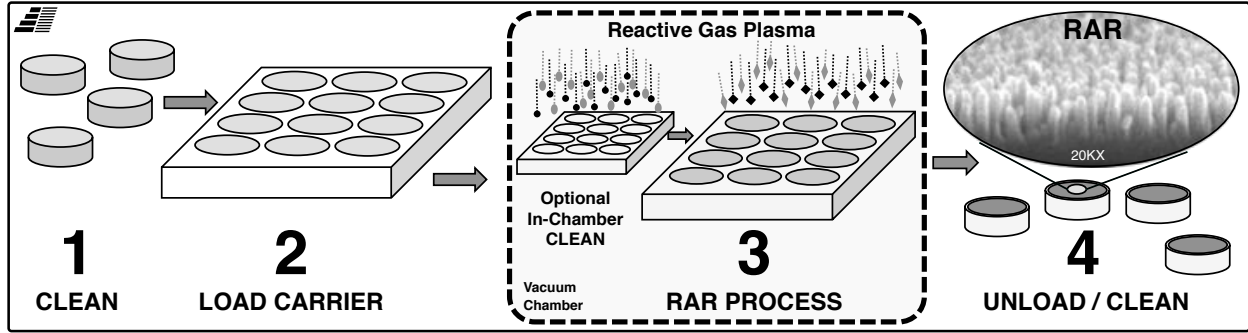
Figure 3: Process flow diagram for the batch fabrication of the RAR texture.

The RAR process was applied to three sub-scale GDS optics supplied by LLNL. Each GDS prototype was a planar fused silica window, 50mm round by 9.5mm thick with a 2μm pitch line grating etched 20nm deep in one surface. Before RAR processing the spectral reflectance of the grating surface was measured over the visible wavelength range to be an average of 3.5% as expected. Figure 4 shows a log-scale plot of the GDS reflection before (dotted black curve) and after (solid grey and solid black curves) RAR texturing. Sample D094 was etched to a greater depth than sample D107 to evaluate the impact on 3ω performance. Higher visible band performance typically results in a lower RAR density that might produce increased 3ω scatter losses. Two dotted lines represent the projected reflectance values at wavelengths below the spectrometer range, estimating less than 0.2% reflectance for two GDS samples at the 3ω wavelength. [The spectrometer employs a single bifurcated fiber optic cable to send and receive a collimated broad-band white light beam from a tungsten-halogen light source. To isolate reflections from just one surface, a backside absorber plate is used consisting of a polished fused silica slab roughened and painted black on one side. The part under test is then placed on the polished surface of the absorber and an index matching fluid (decalin, refractive index n=1.48) is used to couple the transmitted light into the black paint.]

Cross sections of a third GDS witness sample taken by SEM at LLNL, are inset to the Figure 4 plot. The depth of the RAR texture is seen to be more than ten times the 20nm depth of the grating lines, and yet the grating modulation remains. The grating function was verified visually by observing the first order diffracted light from a helium-neon laser before and after RAR processing. Figure 5 shows additional elevation views (45°) of the GDS and superimposed RAR and GDS patterns magnified 9000 times, along with a highly magnified (70,000X) cross section of a single grating step. Note the open nature of the RAR texture features – about 50nm wide at the surface tapering to a point in the valleys. A dashed white line was added to further highlight the grating modulation.
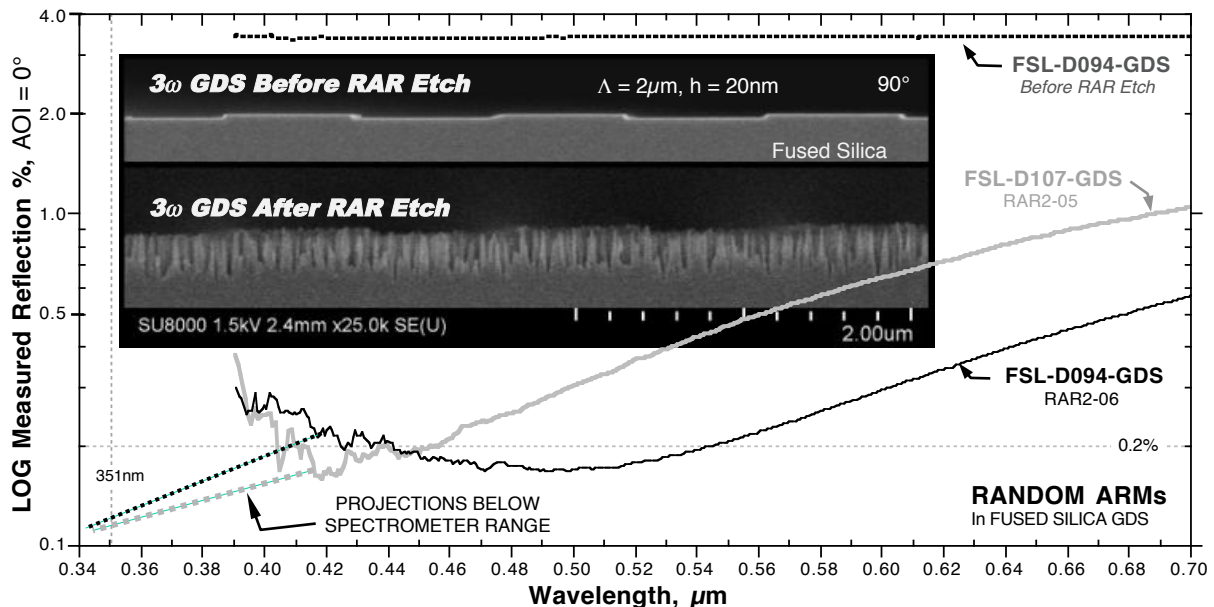

Figure 4: Measured spectral reflectance of GDS samples before and after RAR texture fabrication. Inset: SEM profiles.
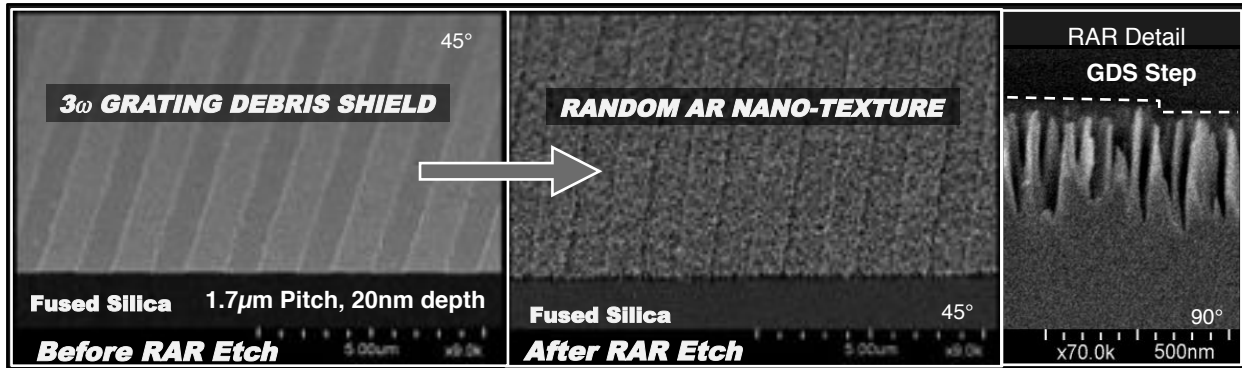
Figure 5: SEM images of a GDS surface before (left) and after (center, right) RAR texture fabrication.

Using a scanning photometer, LLNL measured the efficiency of the GDS samples before and after RAR treatment. Each GDS sample was stepped over a 50 by 50 point grid with a spacing of 1mm to record the spatial uniformity of the transmitted zero and first order diffracted light using a near UV wavelength laser operating at 375nm. Figure 6 gives grayscale plots of this data indicating that the transmitted first order light after RAR treatment remains highly uniform. The average diffraction efficiency within the 40mm circular areas indicated was increased from 0.242% to 0.264% with only a slight change in standard deviation from ±0.0087% to ±0.0098%.
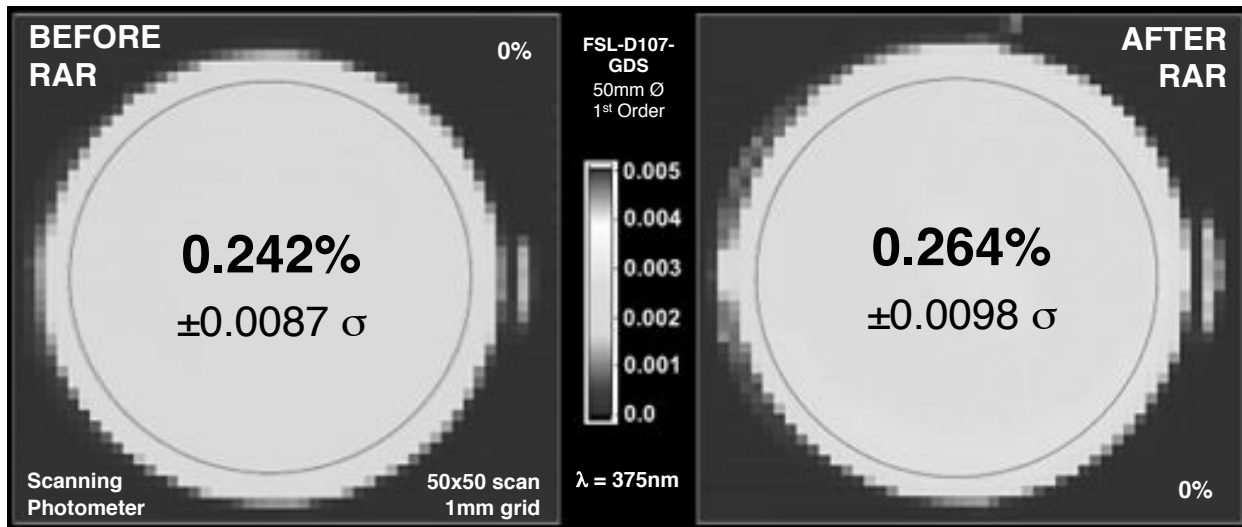

Figure 6: Uniformity of a 1st order diffracted beam from GDS #D107 before (left) and after (right) RAR fabrication.

With the success of the RAR / GDS superposition, additional RAR treated fused silica windows were fabricated for further evaluation in NIF standard pulsed laser damage and hydrocarbon adsorption trials. LLNL supplied three UV grade fused silica laser windows each 50.8mm round by 9.5mm thick. The windows were purchased from CVI Melles Griot with a standard commercial polish specification of 10-5 scratch-dig, 1/10th wave flatness. LLNL then applied their proprietary Advanced Mitigation Process (AMP) that helps to remove residual sub-surface polishing damage and contaminants, and greatly increases the laser damage resistance.[4,5] RAR textures were then etched into one surface of two samples identified as S285 and S395, and in both surfaces of the third sample S410. Figure 7 shows a log-scale plot of the visible-band spectral reflection from one surface of the samples before (dotted black curve) and after (solid grey and solid black curves) RAR texturing. Sample S285 was etched to a greater depth than sample S410 to evaluate the impact on 3ω damage resistance. The data curves are quite similar to those found for the GDS samples in Figure 4 as expected, and a reflectance below 0.2% is projected at 351nm.

Inset within Figure 7 is another grayscale plot of the on-axis transmission through sample S410 measured by LLNL using the scanning photometer described above. The spatial uniformity is again quite high with an average transmission over the 40mm circular area indicated of 99.34%, standard deviation ±0.099%.
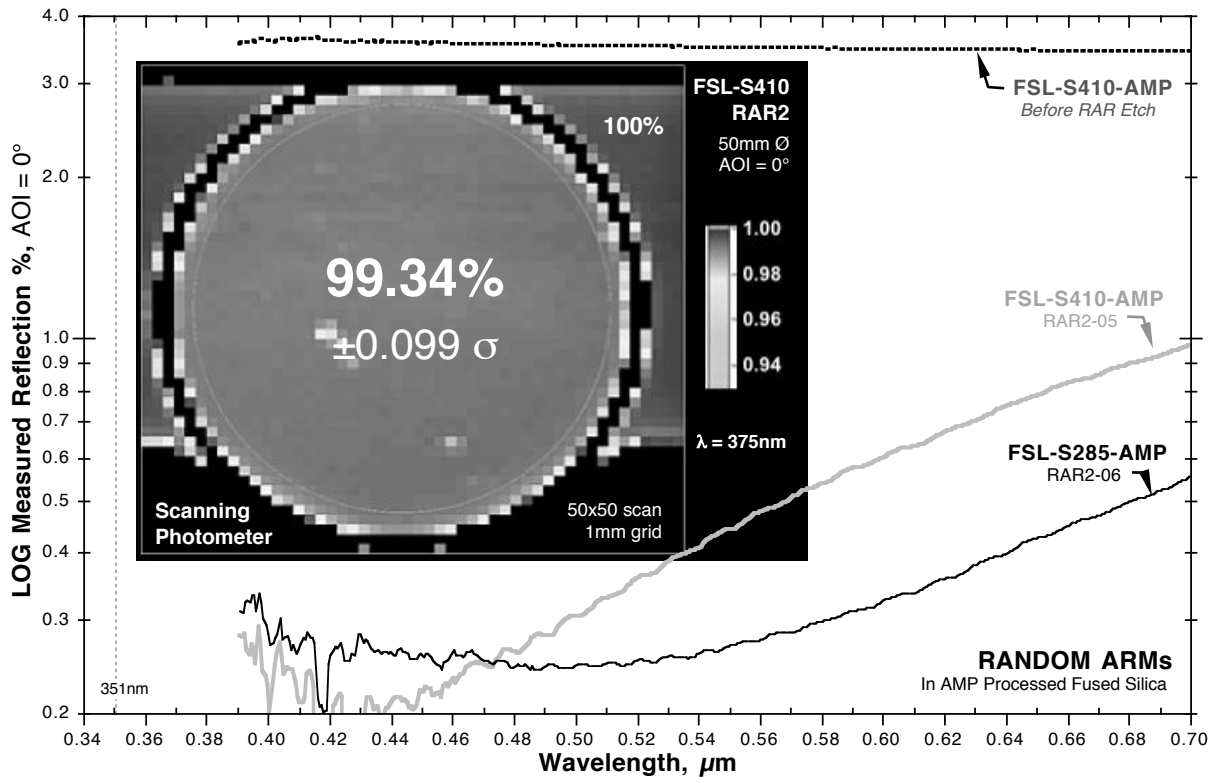
Figure 7: Spectral reflectance of RAR textured fused silica after NIF AMP treatment. Inset: Transmission uniformity.

4.0 VACUUM OUTGAS TESTING – HYDROCARBON ADSORPTION

Sol-gel thin-film AR coatings are used on the fused silica optics at NIF including the second surface of GDS optics. Sol-gel AR coatings eliminate reflection losses and exhibit high laser damage resistance, but the coating layers are porous – susceptible to adsorption of organic compounds that degrade the transmission. The SEM image of a sol-gel layer given in section 2.1 above, shows the tightly packed nature of the silica particles with the space between particles giving rise to the low refractive index. These interstitial voids ('pores') have a dimension in the 5nm range. Hydrocarbons that outgas from materials used within each evacuated FOA at NIF get trapped within these voids leading to a change in the effective refractive index of the sol-gel layer and increased reflection loss.   The contaminated optic must then be removed from the system and the sol-gel coating stripped and reapplied. Because RAR textures have an open surface structure with 50nm features, it was anticipated that hydrocarbon condensation might be less than that found for sol-gel coatings.

To investigate this potential, LLNL subjected RAR textured fused silica sample S410 (Figure 7) to controlled vacuum outgas testing.   Sample S410 was placed in a vacuum chamber along with a fixed concentration hydrocarbon contamination source for an exposure duration of 24 hours. The chamber was held at a temperature of 22C and a pressure of 10^{-6} Torr. Another sample consisting of a 2ω unhardened sol-gel coating layer on both sides of a fused silica window was included as a control that was known to adsorb a significant amount of hydrocarbons in just 24 hours. A second sol-gel sample with NIF baseline ammonia hardened 3ω sol-gel layers coated on both surfaces was also included for direct comparison to the RAR textured sample.   Figure 8 illustrates the three sample
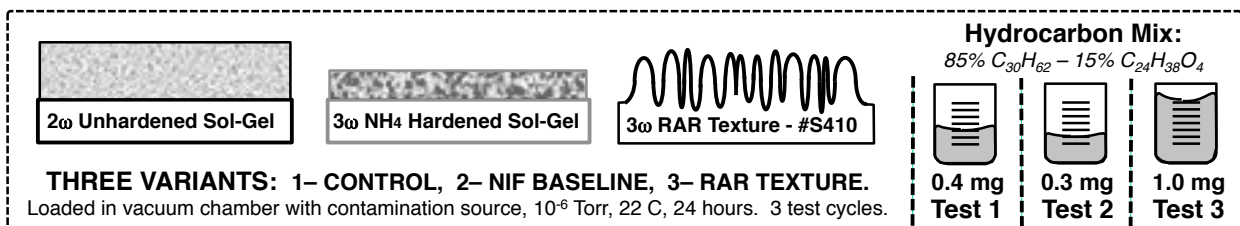

Figure 8: Capillary condensation test conditions and variants.

variants included in each of the three 24-hour exposure cycles. The hydrocarbon contamination source was a mixture by weight of 85% Hexamethyltetracosane, or "Squalane" ($C_{30}H_{62}$), and 15% Dioctyl phthalate, or "DOP" ($C_{24}H_{38}O_4$). The amount of this mixture placed in the chamber was varied from 0.3 milligrams (mg) to 1.0mg.

The transmission of each variant was measured before and immediately after each 1-day exposure cycle, and then rinsed with methylene chloride to collect the adsorbed hydrocarbons for subsequent gas chromatograph, mass spectrometer analysis (GC-MS). This process degrades the sol-gel layer and therefore fresh sol-gel coatings were applied before each exposure cycle. In contrast, the RAR texture durability allowed for an aggressive sulfuric acid and hydrogen peroxide chemical cleaning cycle to be performed after each exposure with no adverse effects on the RAR performance. Figure 9 gives a summary chart of the transmission measurements for all three exposure trials. Significantly, no change in transmission was observed for RAR treated sample S410 at any level of hydrocarbon source concentration. Transmission levels dropped 4.9% for the 2ω control sol-gel sample, and 2.1% for the NIF baseline 3ω sol-gel sample after exposure to the highest hydrocarbon source concentration.
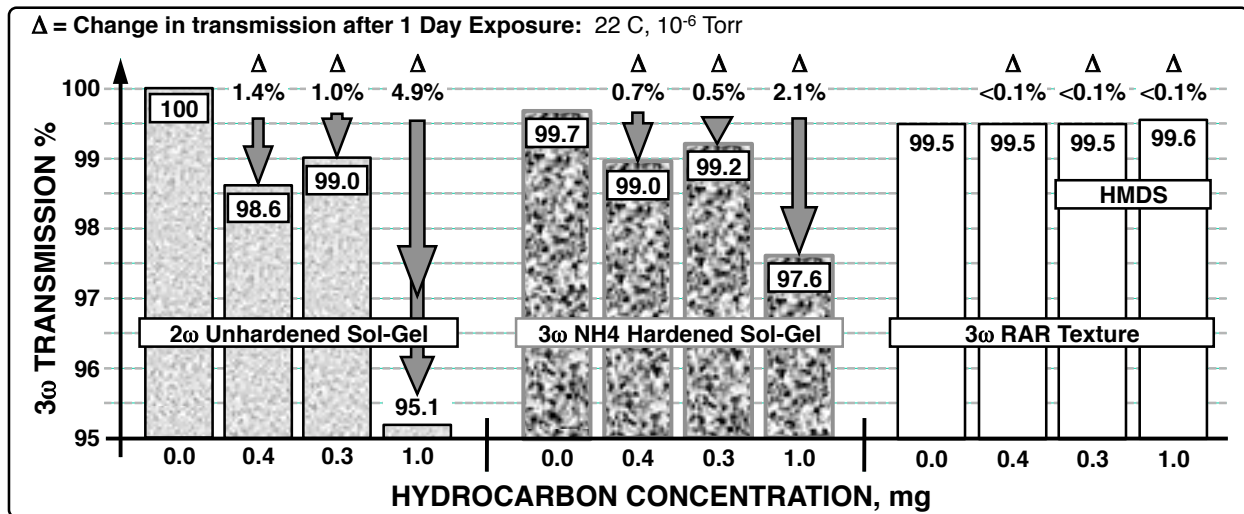

Figure 9: Transmission loss of each variant for a fixed exposure time as a function of hydrocarbon concentration.

The results of the GC-MC analysis showing the number of micrograms (μg) of squalane and DOP adsorbed on the sample surfaces after each exposure cycle, is given in Table 1. After the first exposure cycle with 0.4mg of hydrocarbon, the RAR textured sample adsorbed just 11μg of contaminant, 13 times less than the 143μg adsorbed by the 2ω sol-gel control, and one quarter the amount absorbed by the 3ω hardened sol-gel. The proportion of squalane to DOP for the sol-gel samples was 95% to 5% and 62% to 38% for the 2ω and 3ω samples respectively. The ammonia hardening process produced a significant drop in the sol-gel squalane adsorption, but an increase in the DOP adsorption. For the 3ω RAR sample, 82% of the adsorbed hydrocarbons were DOP. This observation led LLNL to apply a monolayer of hexamethyldisilane (HMDS) to the RAR sample by vapor deposition at a temperature of 100C, a technique common in semiconductor manufacturing. In LLNL's experience, HMDS inhibits

Table 1: Breakdown of hydrocarbon adsorption after each vacuum outgas test cycle.

HYDROCARBON CONDENSATION After 24 Hour, 22C, 1 μT Exposures		TEST 1 25JUL2013			TEST 2* 14AUG2013			TEST 3* 19AUG2013		
#	VARIANT DESCRIPTION	μgrams adsorbed			μgrams adsorbed			μgrams adsorbed		
		SQ	DOP	Total	SQ	DOP	Total	SQ	DOP	Total
1	2ω Unhardened Sol-Gel	136	7	143	90	6	96	270	80	350
2	3ω NH4 hardened Sol-Gel	28	17	45	20	8	28	46	42	88
3	3ω Random AR Nano-Texture	2	9	**11**	0.1	-	**0.1**	0.4	0.1	**0.5**
SQ - "Squalane" $C_{30}H_{60}$ DOP - Dioctyl phthalate $C_{24}H_{32}O_4$ * RAR texture treated with HMDS vapor, 100C, prior to hydrocarbon exposure, Tests 2 & 3 only										

the adsorption of the polar DOP molecules. This proved to be quite effective for eliminating all hydrocarbon adsorption by the RAR treated sample after the second test cycle as shown in the center columns of Table 1. Adjusting for a lower hydrocarbon source amount, the amount and proportion of hydrocarbons adsorbed by the sol-gel samples is nearly the same as is in the first trial, but the RAR sample showed an adsorption of just 0.1μg, a level nearly at the measurement limit. To avoid this lower limit a third test cycle was performed using 3 times the amount of hydrocarbon contaminant. Again the amount of hydrocarbons adsorbed by the sol-gel samples is consistent with the first and second trials, but the amount of hydrocarbons adsorbed by the RAR/HMDS treated sample remains very low - 700 times less than the 2ω control, ~180 times less than the 3ω sol-gel used as the current NIF baseline.

5.0 LASER DAMAGE TESTING

5.1 NIF Baseline pulsed laser damage testing, 351nm, 5ns.

LLNL also conducted a laser damage assessment of the RAR treated fused silica windows of Figure 7 using their Optical Science Laser (OSL) facility. The OSL is a Nd:Glass 10-cm disk amplifier with adjustable pulse width and shape, and an output energy at 351nm of 50 joules per shot at a repetition rate of 2 shots per hour.[21,22] Shots are made in vacuum. RAR treated fused silica window S285 was first mapped using the defect measurement system (DMS), a side illuminated imaging system that catalogs surface defects that scatter light. Figure 10 shows the DMS images taken for S285 before and after pulse testing where the circular regions outline the size of the beam and location of the single shot exposures. Shot area 1 (SA1) was selected for the largest beam exposures to determine the low end of the damage threshold fluence. SA1 showed no damage after two 5ns duration pulses from the OSL at a fluence of 13 J/cm^2. [The OSL pulse is configured to be "flat in time", FIT, gated to have a constant energy over the 5ns pulse duration] To increase the fluence, the OSL beam size was reduced to 9mm diameter (1/e^2) for SA2 and SA3. The fluence was increased to 15 J/cm^2 for one shot at SA2. A small number of damage sites were produced. For the final shot at SA3, the fluence was increased to 18 J/cm^2 producing a large number of point defects that could be counted by the DMS tool.
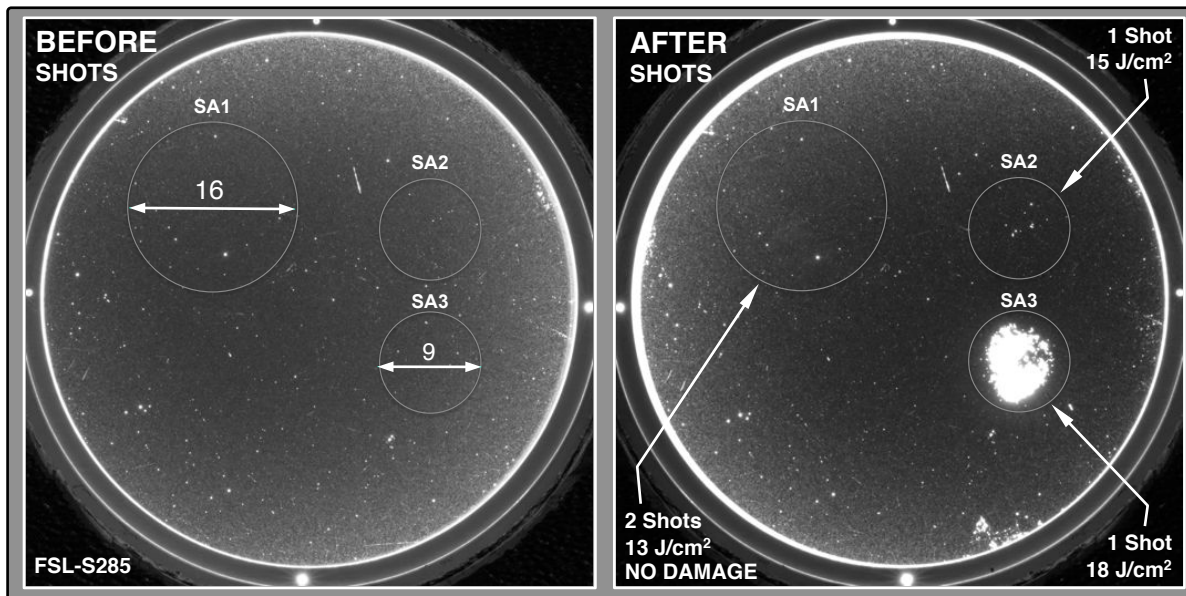

Figure 10: DMS (side illuminated) images showing shot areas before and after testing

Knowing the Gaussian spatial intensity distribution of the OSL beam, the number of defects within a radial zone – the defect density - can be plotted as a function of fluence level. Figure 11 shows such a scatter plot for RAR treated sample S285 indicated (open triangles) compared to the current measured baseline performance of AMP treated fused silica and sol-gel AR coated fused silica optics at NIF (black squares). The damage threshold for S285 is in the 13-14 J/cm^2 range, a bit lower than the 18-19 J/cm^2 range of current NIF optics. The reduced performance of this first trial was likely due to many factors such as prior processing of the window at LLNL, inadequate cleaning and handling procedures at TelAztec after RAR fabrication, or perhaps a RAR texture that was etched too deep targeting visible band performance. This last point may have merit due to the very high threshold values in the 19-20 J/cm^2 range found for the S410 RAR treated samples. Sample S410 was the subject of the multiple hydrocarbon adsorption tests described above, and was aggressively acid cleaned at LLNL prior to the OSL damage test. The issues impacting the damage resistance of RAR treated fused silica, are currently being more carefully sorted out through additional processing trials.
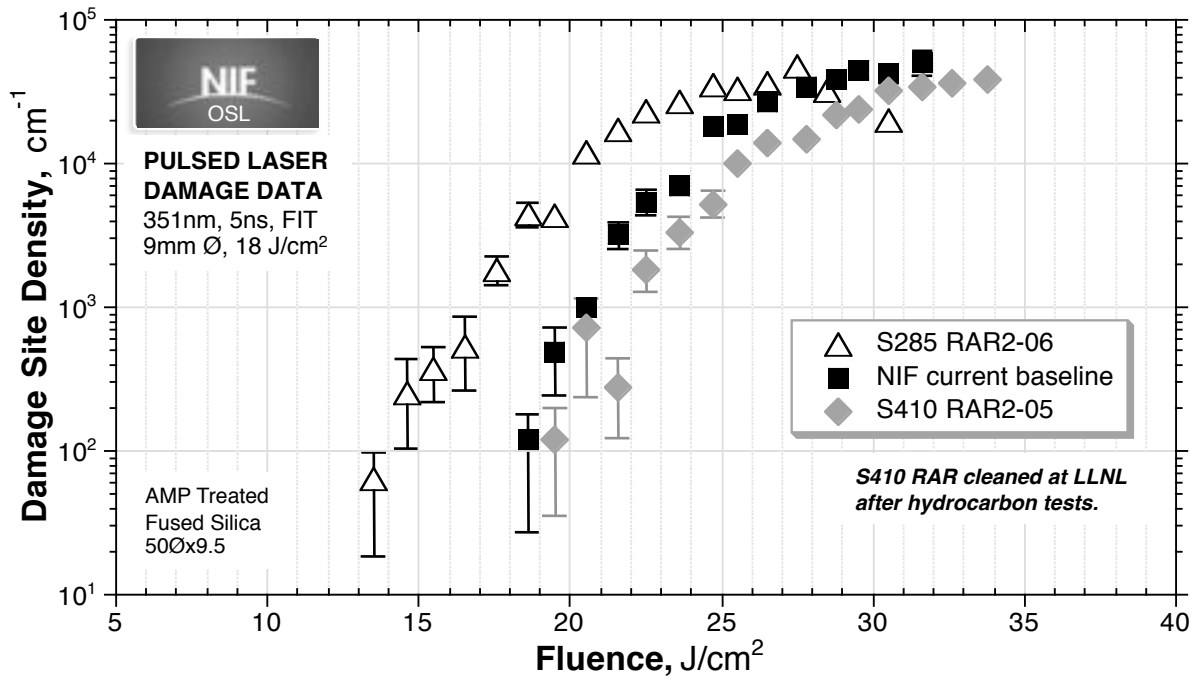
Figure 11: Damage site density as a function of laser fluence for RAR treated fused silica compared to NIF baseline

5.2 Commercial standardized pulsed laser damage testing, 355nm, 10ns.

In an effort to compare the 3ω damage resistance of RAR treated fused silica with conventional thin-film dielectric coatings, a set of fused silica windows were submitted to Quantel USA in Bozeman Montana for their commercial 's-on-1' type pulsed laser induced damage threshold measurements. Quantel's testing adheres to the ISO 11254 standard and involves exposing 100 or more discrete surface sites on a sample to as many as 10 calibrated fluence levels below and above the damage threshold, repeating each fluence level at 10 or more sites. The resulting damage frequency data is then plotted as a function of fluence level with a linear fit to the data determining the threshold. The specific test configuration was: Tripled Nd:YAG laser operating at 355nm wavelength, 10ns pulse width (FWHM), 20Hz pulse repetition rate, 250μm spot diameter $(1/e^2)$, TEM_{00} spatial mode, linear polarization, normal incidence (AOI=0°), 80-120 exposure sites spaced on a grid with >2 time the spot size, 200 shots per site. The criteria for damage is defined as the observation of permanent surface damage under 150X magnification using Nomarski polarized imaging. It is common in fused silica and other glasses under test to observe large scale back surface damage, or blow outs. Often this backside damage occurs without damage to the expose surface and is therefore not included in the damage site count. In fact when such backside damage occurs the pulsing is stopped to avoid propagating the damage over a larger area that might encroach upon the adjacent exposure sites.

A dozen UV grade fused silica windows were submitted to Quantel, all 50.8mm round, between 9.5 and 10mm thick. LLNL supplied 5 AMP treated fused silica windows including one window with NIF baseline ammonia hardened sol-gel AR coatings on both faces. Three of the LLNL windows were RAR treated using two variations of the RAR process dubbed RAR2 and RAR3, and one LLNL window was submitted without any AR treatment (untreated, UT) as a control. A sixth LLNL supplied GDS window with uncertain history was RAR treated and also submitted to the Quantel test. Next, six fused silica windows (Corning 7980) were re-polished to UV laser specifications by a local company (Opticraft, Inc. of Woburn, MA). Three of these six windows were RAR textured using the RAR2 recipe, two were processed with the RAR3 recipe, and one was left as-polished, or untreated (UT) to serve as a control. The resulting visible band spectral reflectance for all samples was similar to that shown in Figures 4 and 7 above. A final detail was that due to the large size of the test samples, all 100 exposure sites could be confined to half the surface area as illustrated in the sketch on the right, potentially allowing a second round of testing.
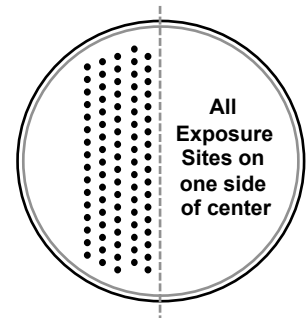
Figure 12 gives a scatter plot of the damage frequency data as a function of the fluence level for 4 of the AMP treated LLNL fused silica windows tested. Consistent with the OSL large beam single-shot tests, the Quantel small beam multi-shot tests show the highest damage resistance for the AMP treated and sol-gel AR coated sample represented by the black squares and dotted black line. Data for the uncoated fused silica sample shown as the open crosses and solid black line, is slightly lower than the sol-gel sample, but the limited number of damage sites found above the zero damage frequency level – a common weakness of the small beam test – may indicate that this difference is not significant. The damage threshold for the two RAR2 processed fused silica windows was averaged to allow for an improved threshold determination. Represented by the grey triangles and solid grey line, the threshold of 26.4 J/cm^2 does appear to be defined sufficiently to suggest that other factors such as cleaning and surface preparation may need to be improved to obtain equivalency with the sol-gel coatings.
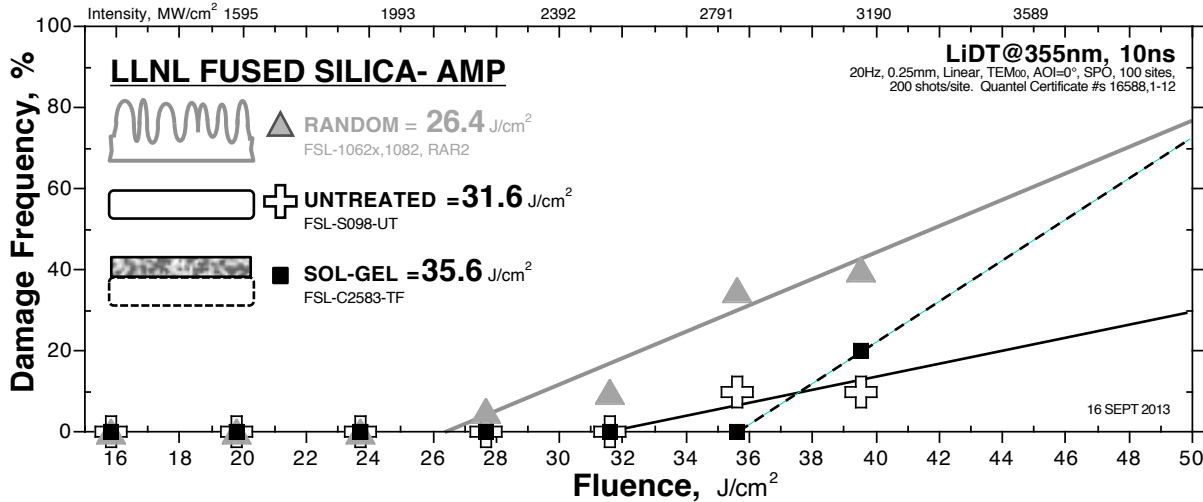

Figure 12: Damage frequency as a function of fluence level for fused silica windows at 355nm, Quantel data.

Figure 13 shows a bar chart comparing the damage thresholds for all 12 windows tested with the 5 AMP treated LLNL windows grouped on the left, and the 6 standard polish fused silica windows grouped on the right. With the exception of the right most data point, it appears that the RAR2 recipe has a higher damage resistance than the RAR3 process. The data also indicates the efficacy of the LLNL AMP treatment that produces damage thresholds about one third higher than the standard polish substrates. A high damage threshold was found for the RAR treated GDS sample represented by the striped bar, a result that needs confirmation with further testing.
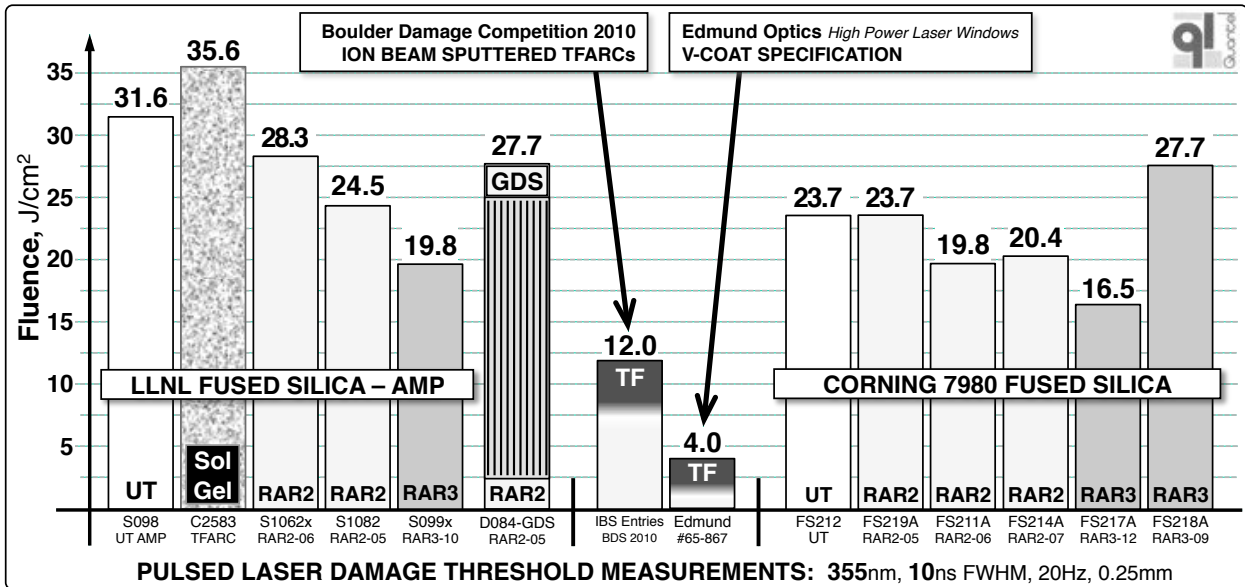

Figure 13: The LiDT of Random ARMs in AMP treated fused silica (left) compared to standard polish fused silica (right).

The damage thresholds for RAR textured fused silica windows are exceptional compared to commercial catalog laser window AR coating specifications. Both Edmund Optics and Newport list the damage threshold of 3ω AR V-coatings at just 4.0 J/cm^2, a level 6 times less than the standard polish RAR treated fused silica windows tested, 8 times less than the AMP treated sol-gel coated windows.[23,24] In addition, the highest performing ion beam sputter (IBS) deposited thin-film coatings tested for the 3ω AR Damage Competition during the 2010 Boulder Damage Symposium, showed a threshold of just 12 J/cm^2, one half to one third the value found for RAR treated windows.[8]

6.0 SUMMARY

RAR nanometer-scale textures have been combined with NIF Grating Debris Shield prototypes to provide a 3.5% transmission boost with no impact on grating function or transmission uniformity. RAR textures were also fabricated in both surfaces of LLNL AMP-processed fused silica windows. A 3ω transmission of 99.5% was obtained with just 0.099% deviation over a 5cm clear aperture. In capillary condensation trials conducted by LLNL, hydrocarbon adsorption on RAR treated fused silica surfaces was found to be two orders of magnitude less than hardened Sol-Gel AR coated surfaces. No RAR sample transmission loss was found 1-day exposure times at multiple hydrocarbon concentrations compared to 0.5% to a maximum of 4.9% loss for the NIF baseline hardened sol-gel AR coated samples. NIF standard large beam size laser damage testing shows a RAR texture damage resistance to be at the same level as the current NIF optics baseline. ISO standard s-on-1 pulsed LiDT tests show a damage resistance 2X higher than IBS TFAR coatings, 5X higher than catalog laser line AR coatings

7.0 ACKNOWLEDGEMENTS

8.0 REFERENCES

[1]   NIF, "Final Optics Assembly," https://lasers.llnl.gov/about/nif/how_nif_works/final_optics_assembly.php
[2]   Wegner, P.J., et.al., "NIF final optics system: frequency conversion…..," Proc. SPIE **5301**, 180 (2004)
[3]   Wegner, P.J., et.al., "National Ignition Facility laser performance: status and thoughts on future capabilities," Proc. SPIE **8885**, 10 (2013)
[4]   Stolz, C.J., et.al., "Engineering meter-scale laser resistant coatings for the near IR…," Proc. SPIE **5963**, (2005)
[5]   Heller, A., "Enhanced Damage Resistance for NIF Optics," LLNL S&T Review, **September**, (2011)
[6]   Thomas, I.M., "Sol-gel coatings for high-power laser optics: past, present …..," Proc. SPIE **2114**, 232 (1994)
[7]   Belleville, P.F., and Floch, H. G., "Ammonia hardening of porous silica …...," Proc. SPIE **2288**, 25 (1994)
[8]   Stolz, C.J., et.al., "BDS Thin Film UV [AR] Laser Damage Competition," Proc. SPIE **7842**, 784206 (2010)
[9]   Thomas, I. M., et.al., "Method for reducing the effect of environmental contamination of sol-gel optical coatings," Proc. SPIE **3492**, 220 (1999)
[10] Britten, J. A., and Summers, L. J., "Multifunction... diffractive structures ...," Appl. Optics, **37**, 3, 7049 (1998)
[11] Rambo, P.K., et.al., "Development of an…. Sol-gel Diffraction Grating," Sandia Report, **045496**, (2004)
[12] Wilson, S.J., Hutley,M.C., "The optical properties of 'moth eye' antireflection surfaces," OpticaActa **29**, (1982)
[13] Lowdermilk, W. H., Milam, D., "Graded-index antireflection….," Appl. Physics Letters, **36** (11), 891 (1980)
[14] Hobbs, D. S., MacLeod, B. D., "Design,... Anti-Reflecting Surface Textures...," Proc. SPIE **5786**, 349 (2005)
[15] Hobbs, D. S., MacLeod, B. D., "Long Life... [AR] Treatment for HgCdTe..," Proc. SPIE **6940**, 69400Y (2008)
[16] Hobbs, D. S., MacLeod, B. D., "Update… Surface Relief Micro-Structures," Proc. SPIE **6545**, 65450Y (2007)
[17] Hobbs, D. S., MacLeod, B. D., "High laser damage threshold surface relief micro-structures for anti-reflection applications," Proc. SPIE **6720**, 67200L (2007)
[18] Hobbs, D. S., "Laser damage threshold measurements…near UV … mid…," Proc. SPIE **7842**, 78421Z (2010)
[19] Hobbs, D. S., MacLeod, B. D., Sabatino, E., "Continued advancement of…," Proc. SPIE **8530**, 85300O (2012)
[20] Hobbs, D. S., et. al., "Automated Interference Lithography Systems for ….," Proc. SPIE **3879**, 124 (1999)
[21] Norton, M.A., et.al., "Growth of laser-initiated damage in fused silica at 351nm," Proc. SPIE **4347**, 468 (2001)
[22] Norton, M.A., et.al., "Determination of laser damage initiation …...," Proc. SPIE **7842**, 784218 (2010)
[23] EdmundOptics, "webpage," http://www.edmundoptics.com/optics/windows-diffusers/laser-line-windows/twentieth-wave-high-power-laser-line-windows/48207
[24] Newport, "webpage," http://search.newport.com/?q=*&x2=sku&q2=10QW20-3